

# Measured stopping powers of $^{12}\text{C}$ and $^{14}\text{N}$ ions in thin elemental foils

D.C. Santry

*Physics Division, National Research Council of Canada, Ottawa, Ontario K1A 0R6, Canada*

R.D. Werner

*Atomic Energy of Canada Limited, Chalk River, Ontario K0J 1J0, Canada*

Received 7 May 1990 and in revised form 7 July 1990

Absolute stopping values for  $^{12}\text{C}$  and  $^{14}\text{N}$  ions in Be, C, Al, Si, Ni, Ag and Au were measured over the energy region 200 to 2000 keV. Surface barrier particle detectors were used to measure the energy loss of heavy ions passing through thin, self-supporting films. The effective charge ratio of heavy ions to hydrogen was examined and found to be a complex function of ion energy and the stopping medium.

## 1. Introduction

In this paper we describe further measurements in our attempt to provide an accurate and consistent set of ion stopping values for some more common elemental materials.

Our studies with the heavier ions  $^{12}\text{C}$  and  $^{14}\text{N}$  provide data for use in radiation damage calculations; for example, in the use of heavy ion beams to simulate neutron damage in nuclear reactor components [1] or in radiation dosimetry where C, N, O and H are the primary recoil products produced in neutron irradiation of tissue [2]. In addition, the data provide useful input for checking theoretical models used to calculate stopping powers.

## 2. Experimental

The experimental conditions used were similar to those described in detail in previous publications [3–5]. Beams of  $^{12}\text{C}$  and  $^{14}\text{N}$  ions were obtained from the CRNL 2 MV National Electrostatics Corporation accelerator and a 2.5 MV Van de Graaff accelerator. As shown in fig. 1, the collimated ion beam strikes a multicomponent target consisting of evaporated layers of Al ( $1.7 \mu\text{g}/\text{cm}^2$ ) or Cr ( $2.2 \mu\text{g}/\text{cm}^2$ ) and Au ( $0.32 \mu\text{g}/\text{cm}^2$ ). A surface barrier particle detector was used to measure the energies of the scattered beams before and after traversing thin elemental films of known thicknesses. The incident beam backscattering at a fixed angle of  $90^\circ$  off each component in the target produces two well defined energies, see fig. 2. A knowledge of the

accelerator energies and the kinematic factors for backscattering provided the energy calibration data for the surface barrier detectors. Such calibrations include corrections for detector window thickness and any nonlinear energy response of the detector. Calibrations were carried out at 100 keV intervals from 200 to 2600 keV relative to the accelerator beam analyzing magnets, which had been calibrated by nuclear threshold reactions. Doubly charged ions from the NEC accelerator were used to cover the energy range 2000 to 2600 keV. Analyzing magnet field values set to produce 2 MeV ions from singly or doubly charged ions did in fact produce identical energies, as measured by the particle detector. Frequent measurements of beam energies

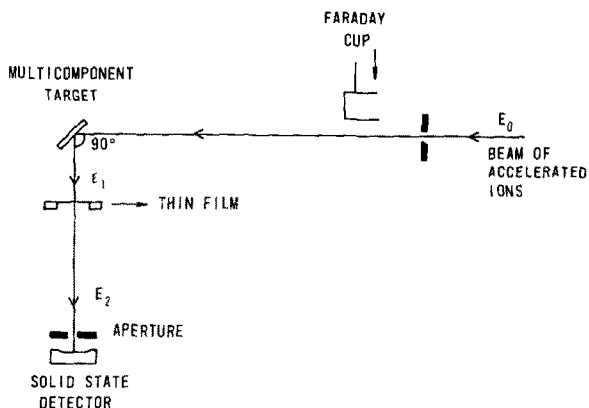


Fig. 1. Experimental arrangement for measuring the energy loss of heavy ions transmitted through thin films.

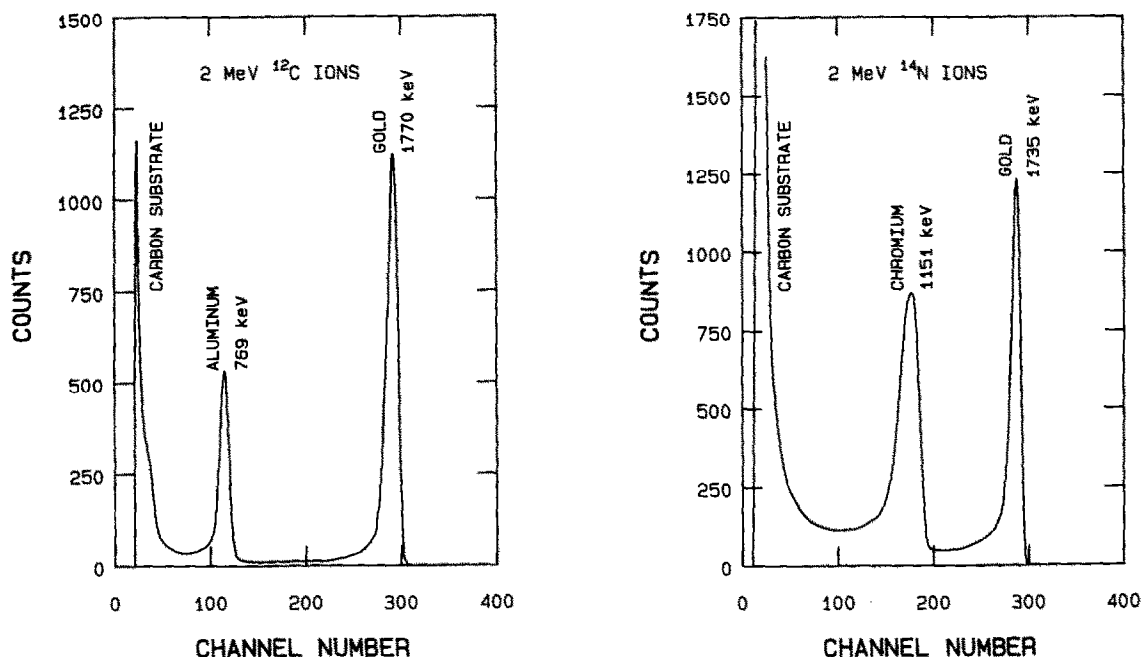


Fig. 2. Pulse height spectra of C and N ions scattered at  $90^\circ$  from thin evaporated layers of Al or Cr and Au on a thick C substrate.

without foils indicated that a well apertured beam was stable to  $\pm 2$  keV.

Thin films were prepared by vacuum deposition. Representative films from each batch prepared were examined by Rutherford backscattering analysis for impurities and homogeneity. Since films of Be, Al and Si readily form oxides during vacuum deposition, it was considered essential to select batches of films with no significant contamination by adsorbed water, oxide formation, carbon deposits or incomplete removal of the release agent. Spectra of the analysis were shown in ref. [6]. A 2 mm diameter  $^4\text{He}$  beam was used to examine various portions of a foil. The energy difference measured between backscattering from front and back surfaces of a film was a constant and indicated that the films were homogeneous over an area of 8 mm by 8 mm

to  $\pm 1 \mu\text{g}/\text{cm}^2$ . Analysis of the films by electron microscopy showed no abnormal structural features for these films. The thicknesses of each film was measured by direct weighing of a known film area ( $\sim 1.3 \text{ cm} \times \sim 1.3 \text{ cm}$ ). During the actual stopping measurements the thicknesses were reconfirmed using a 2 MeV  $^4\text{He}$  ion beam and comparing the observed energy loss with our previously determined  $^4\text{He}$  stopping data [3,4]. For each element, from 10 to 18 different films were used which covered thickness ranges given in table 1. We are careful to express thicknesses as areal density ( $\mu\text{g}/\text{cm}^2$ ) and not ångströms, since the densities of thin films are not known. The many films used were mounted in different orientations normal to the incident heavy ion beams and showed no effects which could be attributed to ion channeling.

The observed energy shift when a film is inserted into an ion beam divided by the known film thickness gives the stopping value for that material.

Table 1  
Thin film characteristics

Film	Thickness range ( $\mu\text{g}/\text{cm}^2$ )	No. of stopping values measured	
		C	N
Be	78-120	43	-
C	28- 48	138	87
Al	53-110	108	42
Si	114-183	152	77
Ni	40- 86	55	68
Ag	55- 98	111	84
Au	69-146	128	81

### 3. Results and discussion

Also listed in table 1 are the number of individual stopping measurements made for each element. A smooth curve drawn through the data points for each element was based on a least squares polynomial fit and the results are shown in figs. 3 and 4. Fitted values at 50 keV intervals are listed in tables 2 and 3. The experimental uncertainty for any of the stopping measure-

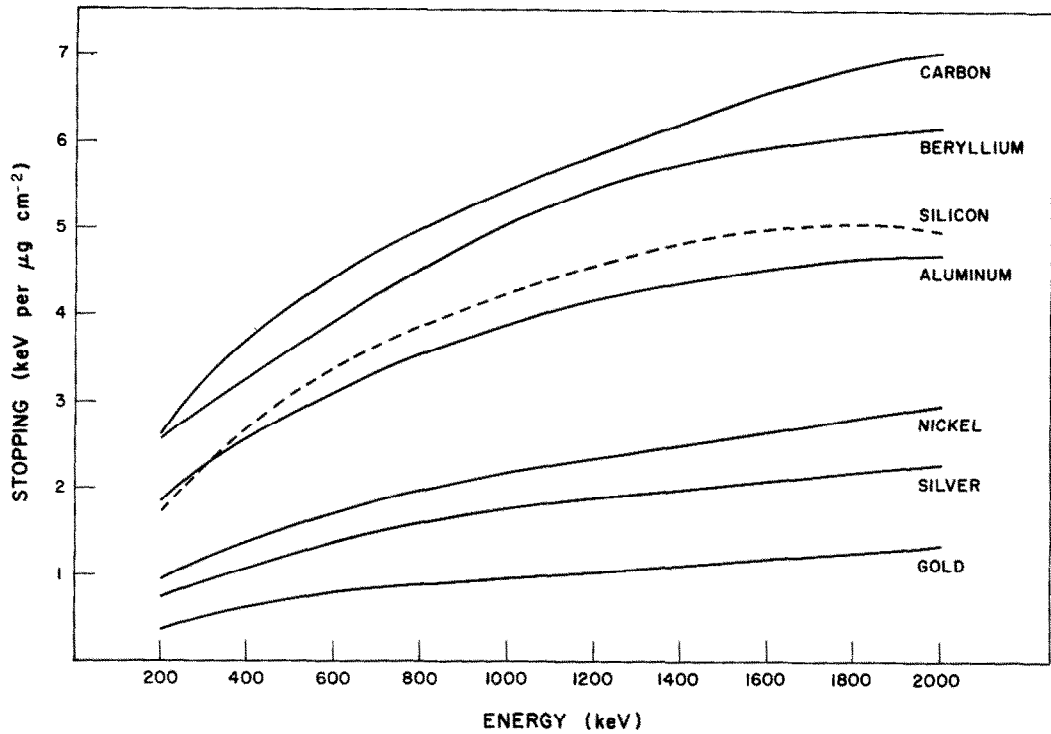


Fig. 3. Energy dependence of stopping values of some elemental films for  $^{12}\text{C}$  ions. The lines represent polynomial least-squares fit to our measured data.

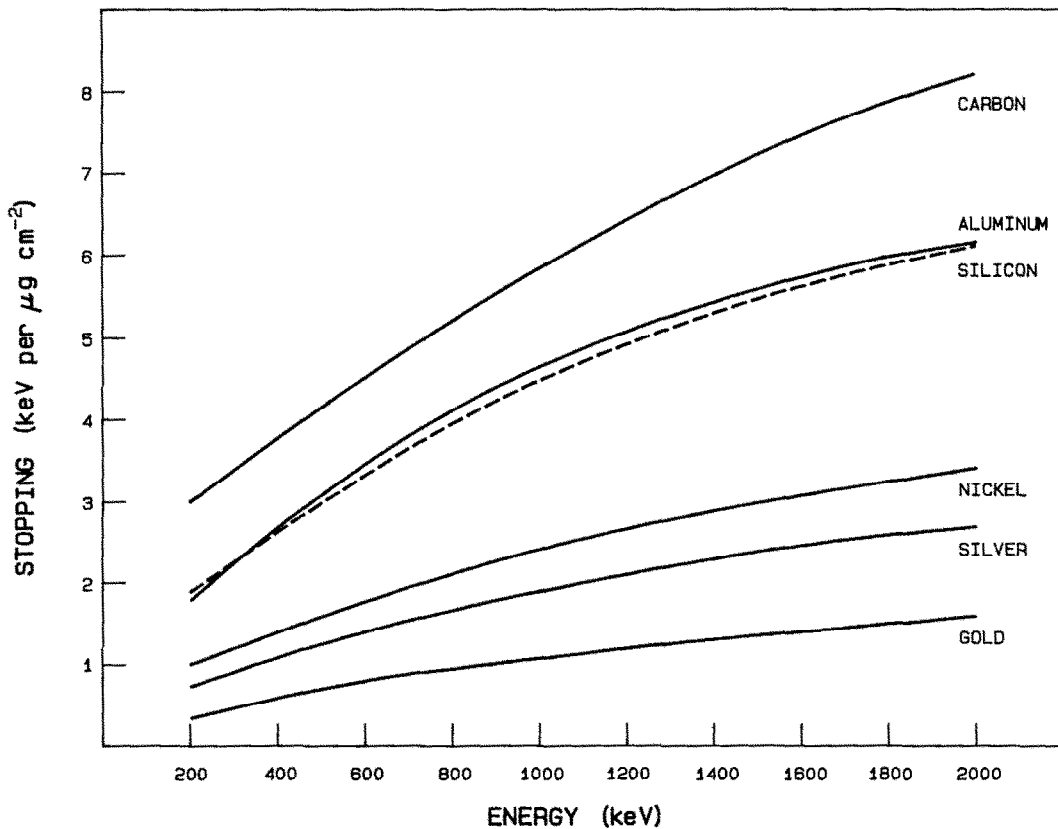


Fig. 4. Energy dependence of stopping values of some elemental films for  $^{14}\text{N}$  ions. The lines represent polynomial least-squares fit to our measured values.

ments consisted of peak fitting to  $\pm 0.2$  channels (0.5 to 1.5%), detector energy calibration and stability (0.2 to 1.0%), film weighing to  $\pm 2 \mu\text{g}/\text{cm}^2$  (0.8 to 3%), and film area determination (2 to 3.5%). The maximum spread in values for a given ion energy was less than 4% so that the estimated uncertainty in the stopping values in tables 2 and 3 is 5%.

In comparing our results with previous measurements we find that the only set of data which cover the energy region of 0.2 to 2.0 MeV were by Porat and Ramavataram [7]. Their results for C ions in C, Al, Ni and Ag are within 0.2 and 8% of our values. The same agreement exists for N ions except for Al where their values at energies above 1 MeV are 13% lower than

ours. Values for C and N ions in Au are 5 to 15% different from ours.

Agreement with other measurements over a limited energy range are as follows: Fastrup et al. [8] 220 to 418 keV C and N ions in C (2 to 7%). Schulz and Brandt [9] 229 to 570 keV N ions in C, Al (0.5 to 8%) and Au (0.2 to 30%). Ward et al. [10] at 202 and 301 keV C ions in C, Ni, Au (6%), Al (15%) and Ag (12%). For N ions at 283 and 340 keV C(5–9%), Al (8–11%), Ni (2–8%), Ag (13%) and Au (1–8%).

It is perhaps more important to compare our measurements with semi-empirical tabulations which were based on existing experimental data, since the latter are generally used rather than individual values from a

Table 2  
Stopping power values for  $^{12}\text{C}$  ions ( $\text{keV}/\mu\text{g cm}^{-2}$ )

Energy (keV)	Stopping materials						
	Be	C	Al	Si	Ni	Ag	Au
200	2.60	2.67	1.87	1.74	0.919	0.718	0.364
250	2.76	2.97	2.07	2.01	1.05	0.819	0.441
300	2.92	3.24	2.25	2.27	1.17	0.913	0.509
350	3.08	3.48	2.42	2.50	1.28	1.00	0.570
400	3.25	3.71	2.58	2.71	1.38	1.08	0.624
450	3.41	3.92	2.73	2.90	1.48	1.16	0.627
500	3.58	4.11	2.87	3.08	1.56	1.23	0.716
550	3.75	4.28	3.00	3.24	1.64	1.30	0.754
600	3.91	4.44	3.12	3.39	1.72	1.36	0.789
650	4.07	4.60	3.24	3.53	1.79	1.42	0.821
700	4.23	4.74	3.35	3.66	1.86	1.48	0.849
750	4.38	4.87	3.45	3.77	1.92	1.53	0.875
800	4.53	4.99	3.55	3.88	1.97	1.58	0.899
850	4.67	5.11	3.64	3.99	2.03	1.63	0.922
900	4.81	5.23	3.72	4.08	2.08	1.67	0.943
950	4.94	5.33	3.81	4.17	2.13	1.71	0.963
1000	5.06	5.44	3.88	4.26	2.18	1.75	0.983
1050	5.18	5.54	3.96	4.34	2.23	1.79	1.00
1100	5.28	5.64	4.03	4.42	2.27	1.83	1.02
1150	5.38	5.74	4.10	4.50	2.31	1.86	1.04
1200	5.47	5.83	4.16	4.57	2.36	1.89	1.06
1250	5.56	5.93	4.22	4.64	2.40	1.92	1.08
1300	5.63	6.02	4.28	4.70	2.44	1.95	1.10
1350	5.70	6.11	4.34	4.76	2.48	1.98	1.12
1400	5.76	6.21	4.39	4.82	2.52	2.01	1.14
1450	5.82	6.30	4.44	4.87	2.56	2.04	1.16
1500	5.87	6.38	4.48	4.92	2.60	2.07	1.18
1550	5.91	6.47	4.53	4.96	2.64	2.09	1.20
1600	5.95	6.56	4.57	5.00	2.68	2.12	1.22
1650	5.98	6.64	4.60	5.03	2.72	2.14	1.25
1700	6.01	6.72	4.63	5.05	2.75	2.16	1.27
1750	6.04	6.79	4.66	5.05	2.79	2.19	1.29
1800	6.06	6.86	4.68	5.06	2.82	2.21	1.30
1850	6.09	6.92	4.70	5.05	2.86	2.23	1.32
1900	6.11	6.97	4.71	5.03	2.88	2.25	1.33
1950	6.14	7.02	4.72	4.99	2.91	2.27	1.35
2000	6.17	7.06	4.72	4.93	2.94	2.29	1.36

Table 3  
Stopping power values for  $^{14}\text{N}$  ions ( $\text{keV}/\mu\text{g cm}^{-2}$ )

Energy (keV)	Stopping materials					
	C	Al	Si	Ni	Ag	Au
200	2.99	1.78	1.86	1.01	0.730	0.340
250	3.19	2.03	2.06	1.11	0.840	0.411
300	3.38	2.27	2.26	1.21	0.942	0.478
350	3.57	2.50	2.45	1.31	1.04	0.541
400	3.76	2.71	2.64	1.41	1.13	0.601
450	3.94	2.92	2.82	1.50	1.21	0.657
500	4.13	3.11	3.00	1.60	1.29	0.710
550	4.31	3.30	3.17	1.69	1.36	0.760
600	4.50	3.47	3.34	1.78	1.43	0.807
650	4.67	3.64	3.50	1.87	1.50	0.851
700	4.85	3.80	3.65	1.95	1.56	0.893
750	5.02	3.96	3.80	2.03	1.62	0.933
800	5.19	4.11	3.95	2.11	1.68	0.971
850	5.35	4.25	4.09	2.19	1.74	1.01
900	5.52	4.38	4.22	2.27	1.79	1.04
950	5.67	4.51	4.35	2.34	1.84	1.07
1000	5.83	4.63	4.48	2.41	1.89	1.10
1050	5.98	4.74	4.60	2.48	1.94	1.13
1100	6.13	4.85	4.71	2.54	1.99	1.16
1150	6.27	4.96	4.82	2.61	2.04	1.19
1200	6.41	5.06	4.92	2.67	2.09	1.21
1250	6.55	5.16	5.02	2.72	2.13	1.24
1300	6.68	5.25	5.12	2.78	2.18	1.26
1350	6.81	5.33	5.21	2.83	2.23	1.29
1400	6.94	5.42	5.30	2.89	2.27	1.31
1450	7.06	5.49	5.38	2.94	2.32	1.34
1500	7.17	5.57	5.46	2.98	2.36	1.36
1550	7.29	5.64	5.54	3.03	2.40	1.38
1600	7.40	5.71	5.61	3.07	2.44	1.40
1650	7.50	5.77	5.68	3.12	2.48	1.43
1700	7.60	5.82	5.75	3.16	2.52	1.45
1750	7.70	5.88	5.81	3.20	2.56	1.47
1800	7.80	5.93	5.87	3.23	2.59	1.49
1850	7.89	5.97	5.93	3.28	2.62	1.52
1900	7.98	6.01	5.99	3.31	2.65	1.54
1950	8.06	6.05	6.05	3.35	2.67	1.56
2000	8.14	6.08	6.10	3.39	2.70	1.59

particular measurement. This enables a reader to judge whether a particular experiment which used stopping values from a tabulation would be expected to give different results if renormalized to our recent data. Northcliffe and Schilling [11] was chosen since their data were used extensively in the 1970s as input to theoretical and experimental works. More recent evaluations are presumably contained in Ziegler's computer program TRIM-88 [12]. The energies chosen in table 4 are those given in Northcliffe and Schilling [11]. Within our experimental uncertainty of 5%, there is fair agreement in the energy region of 200 to 2000 keV for C ions in C, Al and Ni, but only for N ions in Ni and Northcliffe and Schilling [11] values in C.

There are limited energy regions where good agree-

ment exists between our measurements and some of the semi-empirical values. Overall there is no substantial improvement when comparing the 1988 tabulations with those suggested in 1970. This is perhaps not surprising since calculated heavy ion stopping values ( $S_{\text{HI}}$ ) are based on scaling proton stopping values ( $S_{\text{p}}$ ) at the same ion velocity and also requires a knowledge of the effective charge of C and N ions at that ion velocity.

$$S_{\text{HI}} = (Z_{\text{HI}}^*/Z_{\text{p}}^*)^2 S_{\text{p}},$$

where  $Z^*$  represents the effective charge of ions as they slow down in the stopping medium.

Effective charge data in this velocity region cannot be calculated and the data are not generally available

Table 4  
Comparison of stopping values ( $\text{keV}/\mu\text{g cm}^{-2}$ )

Energy (keV)	C ions in stopping materials								
	Be			C			Al		
	a)	b)	c)	a)	b)	c)	a)	b)	c)
300	3.61	4.07	2.92	2.99	3.40	3.24	2.19	2.42	2.25
600	5.04	5.07	3.91	4.23	4.62	4.25	3.08	3.28	3.12
960	6.11	5.75	4.96	5.29	5.70	5.36	3.77	3.09	3.82
1500	6.99	6.21	5.87	6.45	6.69	6.38	4.40	4.28	4.48
1920	7.29	6.33	6.12	7.08	7.07	6.99	4.64	4.44	4.71
	Ni			Ag			Au		
300	1.18	1.13	1.17	0.921	0.866	0.913	0.463	0.461	0.509
600	1.69	1.69	1.72	1.31	1.22	1.36	0.668	0.661	0.789
960	2.13	2.12	2.14	1.66	1.57	1.72	0.872	0.869	0.968
1500	2.58	2.53	2.60	2.02	1.96	2.07	1.11	1.12	1.18
1920	2.80	2.74	2.90	2.18	2.17	2.26	1.22	1.26	1.34

Energy (keV)	N ions in stopping materials								
	Be			C			Al		
	a)	b)	c)	a)	b)	c)	a)	b)	c)
280	3.76	4.36		3.11	3.66	3.30	2.28	2.51	2.18
560	5.30	5.57		4.41	4.92	4.35	3.22	3.54	3.33
980	6.70	6.58		5.73	6.37	5.77	4.12	4.39	4.58
1400	7.59	7.12		6.75	7.38	6.94	4.73	4.85	5.42
1750	9.10	7.41		7.47	7.95	7.70	5.09	5.09	5.88
	Ni			Ag			Au		
280	1.23	1.18	1.17	0.957	0.898	0.902	0.478	0.480	0.452
560	1.76	1.76	1.71	1.36	1.28	1.38	0.686	0.689	0.769
980	2.31	2.36	2.38	1.80	1.73	1.87	0.936	0.949	1.09
1400	2.72	2.76	2.89	2.12	2.09	2.27	1.13	1.17	1.31
1750	2.99	2.98	3.20	2.34	2.33	2.56	1.28	1.33	1.47

a) Northcliffe and Schilling [7].

b) Ziegler [8].

c) This work.

experimentally. If we examine effective charge values obtained from our measurements, as plotted in figs. 5 and 6 (uncertainty of 4%), we see that the effective charge is very dependent on the stopping medium and appears to change with energy in an unpredictable way. These effects were similar to those observed by us in measuring the stopping of  $^7\text{Li}$  ions [5]. Except that the values for effective charge ratios in stopping media were:

$\text{C} > \text{Si} \approx \text{Al} > \text{Ni} > \text{Ag} > \text{Au}$  for  $^7\text{Li}$  ions,

$\text{Si} \gg \text{Al} > \text{Ag} \approx \text{Ni} \approx \text{Au} \gg \text{C}$  for  $^{12}\text{C}$  ions, and

$\text{Al} \gg \text{Si} > \text{Ag} \approx \text{Au} \approx \text{Ni} \gg \text{C}$  for  $^{14}\text{N}$  ions.

Consequently it is difficult with the limited data

available to predict how the effective charge of a heavy ion changes with energy and the stopping medium.

For this reason we have continued our measurements of stopping values for  $^{16}\text{O}$  and  $^{19}\text{F}$  ions. When these data have been processed we shall try to correlate effective charge of an ion as a function of the stopping media and ion energy. In the meantime we have provided another consistent set of measured stopping values for heavy ions in some commonly used target materials. We attempted to establish validity by repeating measurements over and over under the same experimental conditions, then again under different conditions, i.e., different film thicknesses and a different accelerator with an independent energy calibration system. Stopping values were also cross-checked by cycling

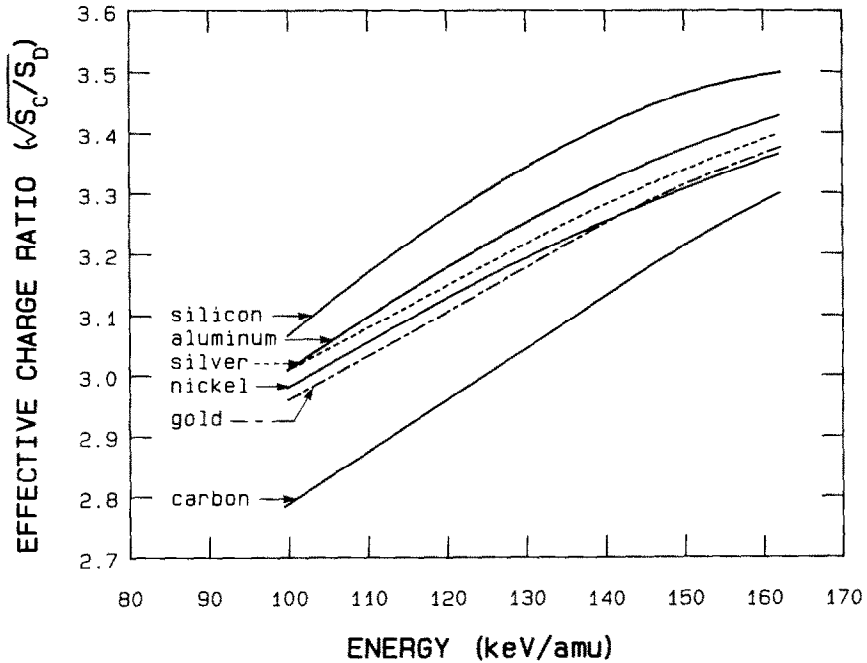


Fig. 5. Energy dependence of the effective charge ratio for  $^{12}\text{C}$  ions based on our measured stopping values for  $^2\text{H}$  and  $^{12}\text{C}$  ions. Estimated uncertainties in the ratios are 4%.

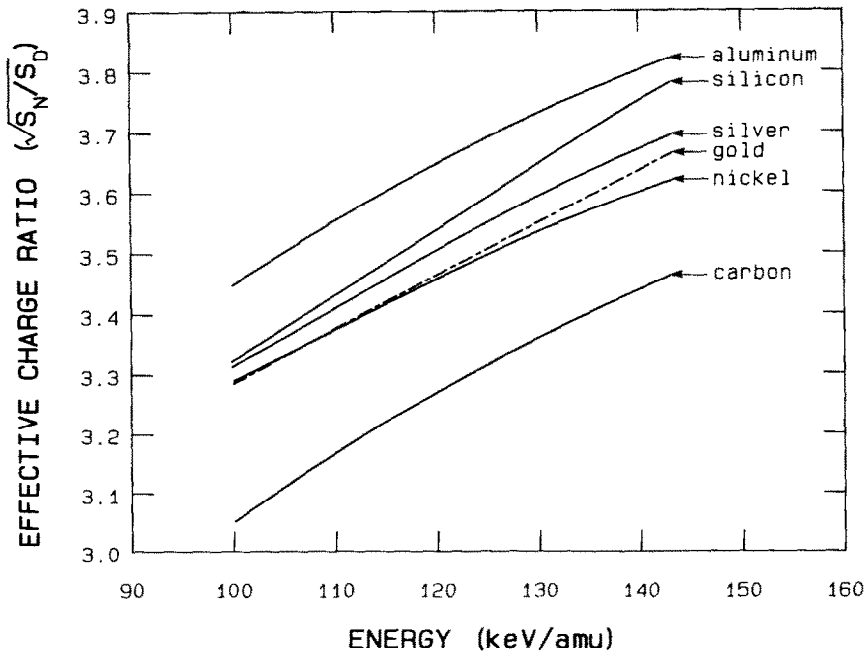


Fig. 6. Energy dependence of the effective charge ratio for  $^{14}\text{N}$  ions based on our measured stopping values for  $^2\text{H}$  and  $^{14}\text{N}$  ions. Estimated uncertainties in the ratios are 4%.

films of different elements under the same experimental conditions. Many of the films had also been used in previous experiments with other heavy ions [3-5].

#### Acknowledgements

We would like to thank J.L. Gallant and P. Dmytrenko for the preparation of high quality thin films and also G.A. Sims for the operation of the accelerators.

#### References

- [1] R.S. Nelson, D.J. Mazey, J.A. Hudson, *J. Nucl. Mater.* (1970) 1.
- [2] M. Inokuti and M.J. Berger, *Nucl. Instr. and Meth.* B27 (1987) 249.
- [3] D.C. Santry and R.D. Werner, *Nucl. Instr. and Meth.* 178 (1980) 523.
- [4] D.C. Santry and R.D. Werner, *Nucl. Instr. and Meth.* 178 (1980) 531.
- [5] D.C. Santry and R.D. Werner, *Nucl. Instr. and Meth.* B5 (1984) 449.
- [6] D.C. Santry and R.D. Werner, *Nucl. Instr. and Meth.* 159 (1979) 523.
- [7] D.I. Porat and K. Ramavatram, *Proc. Phys. Soc. London* 77 (1961) 97 and 78 (1961) 1135.
- [8] B. Fastrup, P. Hvelplund and C.A. Sautter, *K. Dansk. Videnskab. Selskab. Mat.-Fys. Medd.* 35 (1966) no. 10.
- [9] F. Schulz and W. Brandt, *Phys. Rev.* B26 (1982) 4864.
- [10] D. Ward, H.R. Andrews, I.V. Mitchell, W.N. Lennard, R.B. Walker and N. Rud, *Can. J. Phys.* 57 (1979) 645.
- [11] L.C. Northcliffe and R.F. Schilling, *Nucl. Data Tables* A7 (1970) 233.
- [12] J.F. Ziegler, *The transport of ions in matter--TRIM-88* (IBM-Research, Yorktown, New York).